LA-UR-91- 2862

Conf-9108168--1

Los Alamos National Laboratory is operated by the University of California for the United States Department of Energy under contract W-7405-ENG-36.

LA-UR--91-2862

DE92 000314

TITLE: OPTICAL PROPERTIES OF MX CHAIN MATERIALS: AN EXTENDED PEIERLS-HUBBARD MODEL

AUTHOR(S): A. R. Bishop
I. Batistic
J. Tinka Gammel
A. Saxena

SUBMITTED TO: Synthetic Metals

DISCLAIMER

Los Alamos

Los Alamos National Laboratory
Los Alamos, New Mexico 87545

FORM NO. 836 R4
ST. NO. 2629 5/81

Optical Properties of MX Chain Materials: An Extended Peierls-Hubbard Model

A.R. Bishop, I. Batistić, J. Tinka Gammel, A. Saxena
Theoretical Division and Centers for Nonlinear Studies and Materials Science
Los Alamos National Laboratory, Los Alamos, New Mexico 87545

We describe theoretical modeling of both pure (MX) and mixed-halide ($MX_xX'_{1-x}$) halogen (X)-bridged transition metal (M) linear chain complexes in terms of an extended Peierls-Hubbard, tight-binding Hamiltonian with 3/4-filling of *two*-bands. Both inter- and intra-site electron-phonon coupling are included. Electronic (optical absorption), lattice dynamic (IR, Raman) and spin (ESR) signatures are obtained for the ground states, localized excited states produced by impurities, doping or photo-excitation—excitons, polarons, bipolarons, solitons; and the edge states (which occur in mixed-halide crystals, e.g. $PtCl_xBr_{1-x}$). Adiabatic molecular dynamics is used to explore photodecay channels in pure and impure systems for ground states as well as in the presence of pre-existing polaronic states.

71.38+i, 78.30.-j, 71.10.+x

Halogen-bridged transition metal complexes (or MX chains), as well as being important in their own right, provide an important test case for theoretical techniques and issues in low-dimensional materials with strong electron-electron and electron-phonon interactions [1-3]. This is particularly true because of the extreme range of broken-symmetry ground states that are achieved by varying M (Pt, Pd, Ni) and X (Cl, Br, I, etc.) as well as ligands, pressure, magnetic field—ground states ranging from a strongly disproportional CDW (e.g. PtCl) to a weak CDW (e.g. PtI) to SDW or spin-Peierls (and other mixed CDW/SDW [4]) phases (e.g. NiBr, NiCl), in addition to long-period "superlattice" structures [5].

Theoretically, we have used an Hartree-Fock (H-F) spatially inhomogeneous mean-field approximation (MFA) to study the electronic structure [3] and a direct-space random phase approximation (RPA) to investigate phonons [6] (and associated infrared and Raman spectra) in appropriate many-body Hamiltonians. With parameter input from local-density functional [7] and *ab initio* quantum chemistry calculations [8], and comparisons with experiments [1,9], we have employed many-body techniques including H-F, exact diagonalization and adiabatic molecular dynamics to explore the ground and excited states. Agreement between predicted optical, ESR, infrared (IR) and resonance Raman (RR) spectra with recent experiments [1,9,10] on both the pure and mixed-halide MX chains has been quantitatively achieved.

We have modeled effective isolated single chains of pure MX materials in terms of a 3/4-filled, 2-band Peierls extended-Hubbard model. In the case of an isolated mixed-halide chain [11] we replace a segment, containing m X atoms, by X′ atoms where X,X′=Cl, Br, I. Focusing on the metal d_{z^2} and halogen (X,X′) p_z orbitals and including only the nearest neighbor interactions we construct the following tight-binding many-body Hamiltonian [2,3]:

$$H = \sum_{l,\sigma}\Big\{(-t_0+\alpha\Delta_l)(c^\dagger_{l,\sigma}c_{l+1,\sigma}+c^\dagger_{l+1,\sigma}c_{l,\sigma}) + [\epsilon_l-\beta_l(\Delta_l+\Delta_{l-1})]c^\dagger_{l,\sigma}c_{l,\sigma}\Big\} + \sum_l U_l n_{l\uparrow}n_{l\downarrow} + \frac{1}{2}\sum_l K_l\Delta_l^2 + \frac{1}{2}K_{MM}\sum_l(\Delta_{2l}+\Delta_{2l+1})^2 \,, \tag{1}$$

where $c^\dagger_{l,\sigma}$ ($c_{l,\sigma}$) denotes the creation (annihilation) operator for the electronic orbitals at the lth atom with spin σ. M and X(or X′) occupy even and odd sites, respectively. $\Delta_l := \hat{y}_{l+1} - \hat{y}_l$, where $\hat{y}_l$ are the displacements from uniform lattice spacing of the atoms at site l. Equation (1) includes as parameters the onsite energy ϵ_l ($\epsilon_{2l} = \epsilon_M = e_0$; $\epsilon_{2l+1} = \epsilon_X = -e_0$ in the X region and $\epsilon_{2l+1} = \epsilon_{X'} = e_0 - 2e'_0$ in the X′ region, ϵ_i being the electron affinity of the ith ion), electron hopping (t_0, t'_0), on-site ($\beta_M, \beta_X, \beta'_X$) and inter- site ($\alpha, \alpha'$) e-p coupling, on site e-e repulsion (U_M, U_X, U'_X), and finally effective M-X (K) or M-X′ (K′) and M-M (K_{MM}) springs to model the elements of the structure not explicitly included. In particular, (K_{MM}) accounts for the rigidity of the metal sublattice connected into a 3-dimensional network via ligands. Long-range Coulomb fields are also included when necessary (as in strongly

valence localized cases). Note that the metal M=Pt energies ϵ_{2l} are the same in the segment and the host MX chain. At stoichiometry there are 6 electrons per M_2X_2 (or M_2X_2') unit, or 3/4 band filling. A combination of ground state experimental data (the X-sublattice distortion amplitude Δ_0, the $\sigma(X) \rightarrow d\sigma^*$ absorption for the oxidized monomer, and the inter-valence charge transfer (IVCT) band edge, E_g, quantum chemical calculations [8] have lead us to the effective parameter sets for the Hamiltonian of Eq. (1) listed in Table 1.

In the following we present selected results from our comprehensive study for both the pure [3] and mixed-halide [11] MX chains.

Fig. (1) depicts calculated ESR spectra for polarons on a PtBr chain. Fig. (1a) shows an electron polaron centered on an oxidized metal atom ($Pt^{3+\delta}$) while in Fig. (1b) a hole polaron is centered on a reduced metal atom ($Pt^{3-\delta}$). Since PtBr is a weakly localized CDW system, electron spin density is spread over several sites. Multiple peaks in the ESR spectra are a result of hyperfine splitting due to the interaction between electron and nuclear spin. In the present illustrative calculations we have taken the matrix element for electron-nuclear spin interaction to be the same for both Pt and Br. However, once we include the appropriate matrix elements for Pt and Br we expect the amplitude of the hyperfine structure in Fig. (1) to be reduced. Note the electron and hole asymmetry in the ESR spectra which is consistent with experimental data [1,10] and is a consequence of the two-band nature of our model (i.e. explicit inclusion of the 4 atoms of the unit cell).

We have also investigated the photodecay channel subsequent to photoexcitation in the ground state as well as in the presence of nonlinear excitations and impurities using adiabatic molecular dynamics [3]. Photoexcitation was simulated numerically by manually removing an electron from an occupied state and instantaneously placing it in an unoccupied state. The system was allowed to evolve adiabatically with no further changes in electronic occupations. Fig. 2 shows the evolution of PtBr after a single electron is photoexcited across the Peierls gap, with the addition of the gap energy (E_g) to the system. As is clear from Fig. 2(a), initially an exciton is formed within a phonon period. However, this exciton is unstable and evolves into a slowly separating kink-antikink pair. The electronic occupancies of the excited state necessitates that both of these kinks are neutral. Since the creation energy of the kink-antikink pair is smaller than the gap energy, the remaining energy goes partly into the kinetic energy of the kinks, partly into the acoustic phonons and partly in the form of a small amplitude localized "breather" (phonon bound state) between the kinks. Such a breather, a temporally and spatially coherent state of optical phonons, is clearly visible in Fig. 2(a). Fig. 2(b) shows the time evolution of associated energy levels, in particular the characteristic gap states of a kink pair. within ~200 femtoseconds two continuum states are pulled into one (almost) degenerate midgap state indicating that the initial bound electron hole pair (exciton) quickly evolves into a kink-antikink pair. At the same time a breather level oscillates about the conduction band edge into the gap and persists with a time period larger than the phonon period. Investigations

of the influence of impurities on this photodecay channel are in progress.

Next we illustrate a few salient features of mixed-halide chains [9,11] by way of predicted optical, infrared (IR) and resonance Raman (RR) spectra. In Fig. (3) a PtCl chain of length N=48 atoms is considered in which a segment containing 8 Cl atoms is replaced by Br atoms. The interface (edge) between the PtCl and PtBr segments is on a reduced metal site ($Pt^{3-\delta}$). Fig. 3(a) depicts the optical absorption for such a mixed-halide chain. Note that in addition to the two peaks at 1.5 eV and 2.5 eV, which correspond to the inter-valence charge transfer (IVCT) energy for PtBr and PtCl, respectively, there are absorption peaks between the two IVCTs (intragap) as well as several peaks beyond 2.5 eV (ultragap). These extra peaks arise from the strong mixing of the electronic bands of the two kinds of chains in the electronic spectrum (not shown).

We have identified local *phonon* modes associated with the edge in the mixed-halide chains that correlate directly with the measured RR spectra [9] and the electronic resonance energies of Fig. 3(a). Fig. 3(b) shows the calculated IR spectra for the mixed-halide ($PtCl_{.67}Br_{.33}$) chain. The peak at 349 cm^{-1} corresponds to the PtCl IR mode while the peak at 239 cm^{-1} corresponds to the PtBr IR mode. Fig. 3(c) shows the predicted RR spectra for three different excitation energies. At an excitation energy 1.5 eV, which is about the same as the PtBr IVCT, the PtBr Raman mode at 172 cm^{-1} is prominent. Similarly, when the excitation energy is 2.55 eV, which is approximately equal to the PtCl IVCT, the PtCl Raman mode becomes resonant at 308 cm^{-1}. However, at an intermediate excitation energy (2.0 eV) several other localized modes become resonant. Fig. 3(c) shows that apart from the pure PtCl and PtBr modes at 308 cm^{-1} and 172 cm^{-1} a mode at 225 cm^{-1} becomes very prominent. This mode arises from the interface between the two differing segments. We label it as the *edge* mode [9]. The peaks at low frequency arise from the acoustic branch of the RPA phonon spectrum (not shown). We emphasize that different local modes become Raman active at different excitation energies and their relative intensities also vary. The excitation profile for various Raman active modes (not shown) is consistent with the optical absorption shown in Fig. 3(a).

In conclusion, we have given a brief overview of the important optical probes in both the pure and mixed-halide MX chain solids. We have also studied the isotope effect in terms of IR and RR signatures in these systems. Furthermore, we are also beginning to explore mixed-metal ($M_xM'_{1-x}X$) and bimetallic (MMX) systems, as well as effects of magnetic fields (especially on the weak CDW/SDW ground state materials [4]). While, on one hand, we believe that the MX *class* of compounds are nearly uniquely important as a testing ground for many-body modeling and materials design strategy in strongly correlated, low-D materials, we are on the threshold of investigating their technologically important applications on the other. Indeed, doping and photoexcitation studies of mixed-halide systems [12] indicate that electron and hole defects preferentially locate on differing chain segments (i.e. holes in the PtCl segemnt, electrons in the PtBr segment). This points to photovoltaic device

applications of the mixed-halide single crystals. Since the electronic and spectroscopic properties of MX crystals depend very sensitively on the presence and nature of a variety of impurities, counterions, and ligands, they are very good prospects for chemical sensors (or so called electronic-noses).

We acknowledge important discussions with R. Donohoe, X.Z. Huang, B. Swanson and L. Worl. This work was supported by the US DOE.

REFERENCES:

(1) These proceedings and Proceeding of the ICSM '90, Tübingen, Germany, Synth.Met.**41-43**, (1991).

(2) J.T. Gammel, R.J. Donohoe, A.R. Bishop, and B.I. Swanson, Phys. Rev. B **42**, 10566 (1990).

(3) J.T. Gammel, A. Saxena, I. Batistić, A.R. Bishop, and S.R. Phillpot, Phys. Rev. B (1991), preprint.

(4) H. Röder, J.T. Gammel and A.R. Bishop, preprint.

(5) I. Batistić, J.T. Gammel and A.R. Bishop, Phys. Rev. B, preprint.

(6) I. Batistić and A.R. Bishop, Phys. Rev. B (1991).

(7) R.C. Albers, Synth. Metals **29**, F169 (1989);R.C. Albers, M. Alouani, J.M. Wills, and M. Springborg, Synth. Metals **41/3**, 2739 (1991);M. Alouani and R.C. Albers, unpublished.

(8) C. Boyle, R. L. Martin, and P. J. Hay, unpublished.

(9) B.I. Swanson, et al., Synth. Met. **41**, 2733 (1991); Mol. Cryst. Liq. Cryst. **194**, 43 (1991).

(10) S. Kurita and M. Haruki, Synth. Met. **29**, F129 (1989); M. Tanaka and S. Kurita, J. Phys. C **19**, 3019 (1986).

(11) A. Saxena, X.Z. Huang, I. Batistić, A.R. Bishop, L.A. Worl, and B.I. Swanson, Phys. Rev. B, in preparation.

(12) L.A. Worl, S.C. Huckett, B.I. Swanson, A. Saxena, A.R. Bishop, and J.T. Gammel, Phys. Rev. Lett., preprint.

TABLES

TABLE I. Parameters for the PtX materials in Eq. (1). $\beta_X = -0.5\beta_M$.

MX	t_0 (eV)	α (eV/Å)	e_0 (eV)	β_M (eV/Å)	K_{MX} (eV/Å^2)	K_{MM} (eV/Å^2)	U_M (eV)	U_X (eV)	Δ (Å)	E_g (eV)
PtCl	1.02	0.5	2.12	2.7	6.800	0.0	1.9	1.3	0.38	2.50
PtBr	1.26	0.7	0.60	1.8	6.125	0.7	0.0	0.0	0.24	1.56

FIGURE CAPTIONS:

1. The calculated ESR spectrum for (a) an electron polaron and (b) a hole polaron on a PtBr chain.

2. Dynamics of photoexcitation in PtBr: (a) CDW distortion as a function of time in units of 10^{-15} seconds, and (b) energy levels as a function of time for photoexcitation of the ground state.

3. Theoretical (a) optical, (b) infrared (IR) and (c) resonance Raman (RR) spectra for a mixed-halide chain composed of a segment of 8 Br in a chain of total length 48. Notice the resonance effect in Raman as the excitation energy is tuned through the local "edge" levels. Intensity scales here are in arbitrary units.

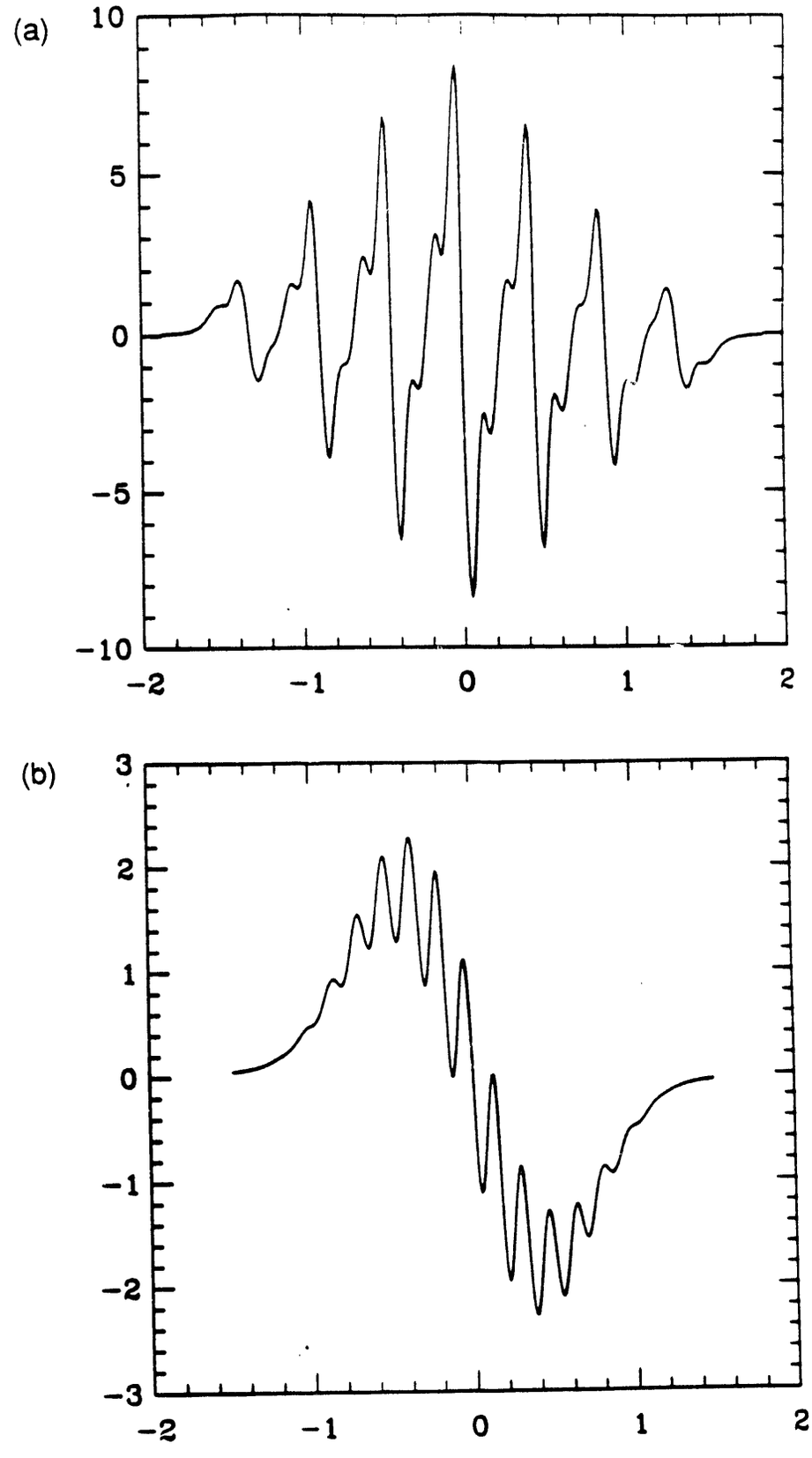

Fig. 1

(a)

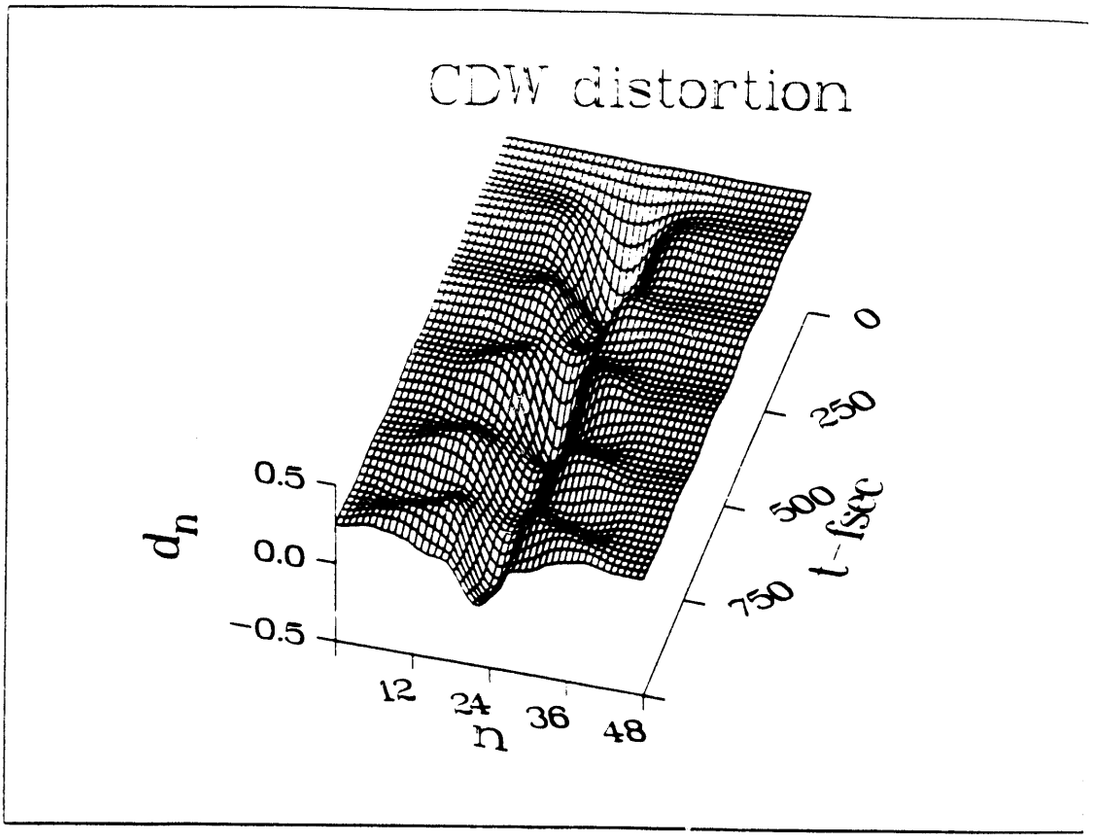
CDW distortion
d_n
0.5
0.0
-0.5
12
24
36
48
n
0
250
500
750
t - fsec

(b)

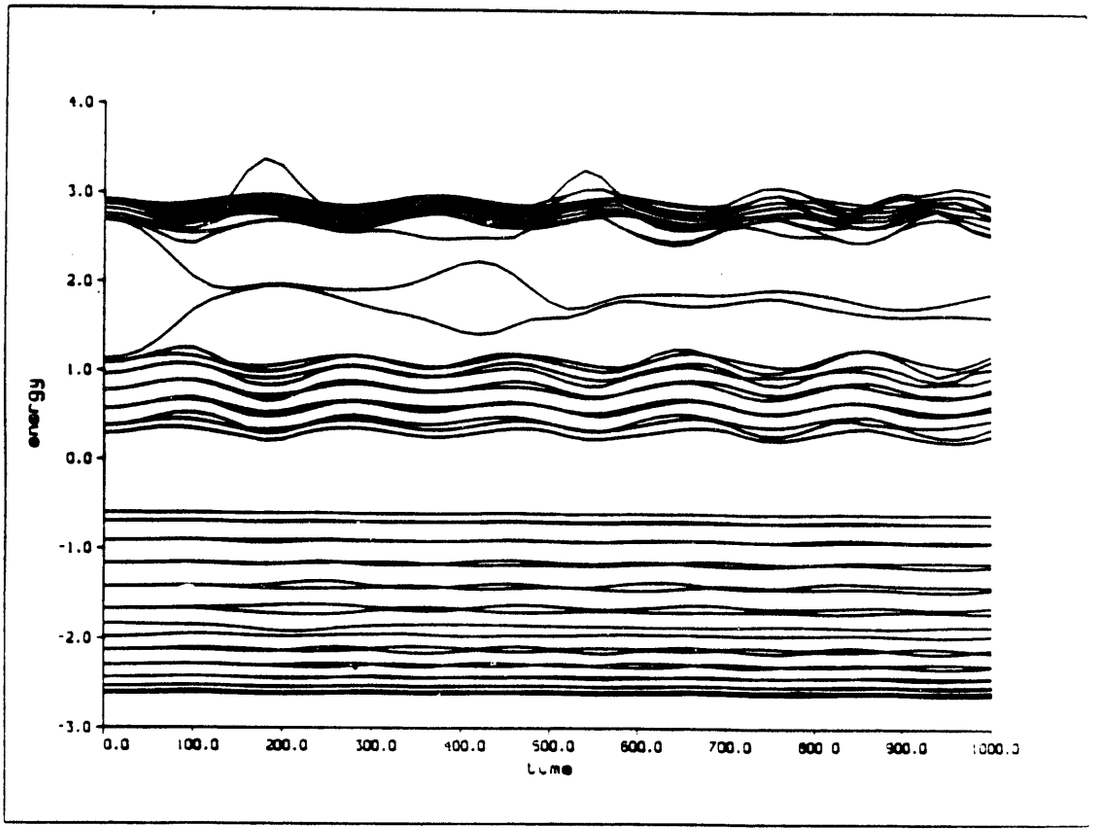
energy
4.0
3.0
2.0
1.0
0.0
-1.0
-2.0
-3.0
0.0
100.0
200.0
300.0
400.0
500.0
600.0
700.0
800.0
900.0
1000.0
time

Fig. 2

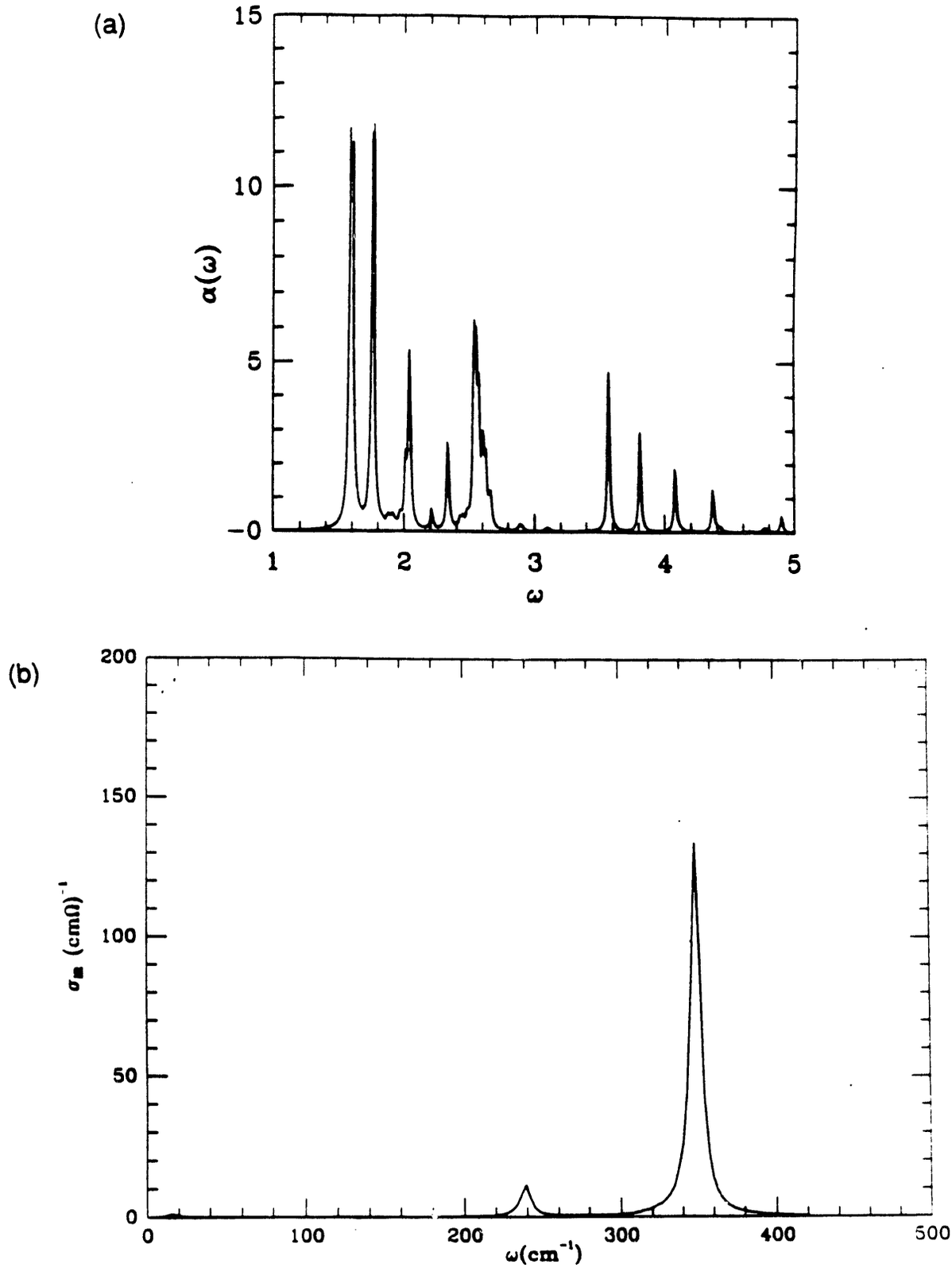
(a)
15
10
5
0
α(ω)
1
2
3
4
5
ω
(b)
200
150
100
50
0
σ (cmΩ)⁻¹
0
100
200
300
400
500
ω(cm⁻¹)

Fig. 3

(C)

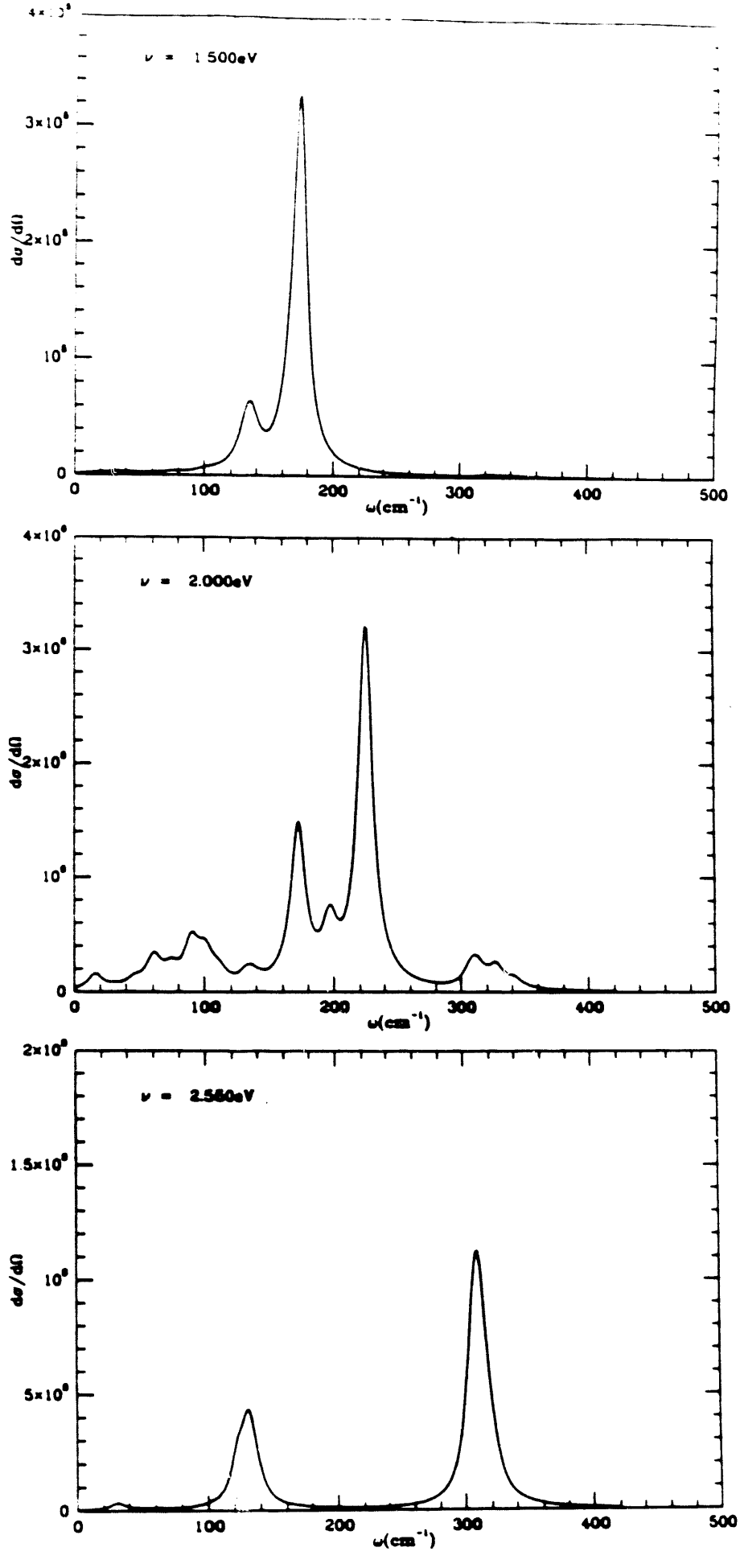

END

DATE FILMED

10 / 29 / 91